Synthesis and characterization of a porous amorphous Ni–B catalyst on titania by silver-catalyzed electroless plating†

Zhijie Wu, Minghui Zhang,* Shaohui Ge, Zhili Zhang, Wei Li and Keyi Tao

Received 2nd August 2005, Accepted 19th September 2005
First published as an Advance Article on the web 6th October 2005
DOI: 10.1039/b510975b

An amorphous Ni–B/TiO_2 catalyst has been synthesized by silver-catalyzed electroless nickel plating. The amorphous structure of Ni–B nanoparticles was characterized by X-ray diffraction (XRD) and selected area electron diffraction (SAED). A transmission electron micrograph (TEM) of the Ni–B/TiO_2 showed particles with size ranging from 30 to 50 nm were homogeneously dispersed over TiO_2 support. High-resolution transmission electron microscopy (HRTEM) indicated that the Ni–B nanoparticles presented a porous and flower-like morphology, which was different from the solid sphere of conventional Ni–B particles prepared by impregnation–reduction method. To investigate the formation process of the porous Ni–B particles, the diffusion of nickel nuclei and the growth of Ni–B particles were characterized. The as-prepared porous Ni–B/TiO_2 catalyst exhibited superior catalytic activities in the hydrogenation reactions to those of catalysts prepared by conventional methods.

Introduction

Interest in amorphous alloys has experienced resurgence internationally over the past 50 years largely spurred by their unique electronic, magnetic and surface properties and their increasing utility in a broad range of application.[1–4] Recently, amorphous alloys have gained increasing attention as novel catalytic materials, with the unique combination of small particle size and short-range ordering and long-range disordered structure.[5–10] Most often they are excellent catalysts in hydrogenation reactions. For example, amorphous nickel alloys exhibit excellent catalytic activity and selectivity equivalent or superior to those of conventional catalysts in various hydrogenations.[11,12] If the amorphous Ni–B nanoparticles are on the support with larger surface area, it is significant to prepare amorphous alloy catalysts for industrialization.[13–15] Alternatively, it is urgent to find an promising way to prepare amorphous alloy catalysts with larger surface area and higher thermal stability. The chemical preparation of bulk and supported Ni–B alloy by reducing nickelous aqueous solution or nickel salt impregnated on support with potassium borohydride has been studied frequently.[11–16] However, the conventional preparation is sensitive to the process of impregnation and reduction of nickelous ions, during which the utility of nickelous ions is poor.[13] Therefore, it is significant to develop an easy and effective synthesis method for preparing amorphous Ni–B alloy catalysts.

In order to design amorphous alloy catalysts for catalytic hydrogenation, one is challenged by the need to control the dispersion of active sites on the surface. Among the various methods for the synthesis of amorphous alloys, electroless nickel (EN) plating technology has been widely used in preparing amorphous films for corrosion resistance.[17–19] EN plating is characterized by the selective reduction of nickelous ions at the surface of a catalytic substrate immersed in an aqueous solution of nickelous ions, with continuous deposition on the substrate through the autocatalytic action of the deposit itself. As the EN plating solution is a kinetically stabilized system, a few types of metals that possess catalytic activity for the plating solution should be firstly deposited on the surface of non-catalytic substrates.[20,21]

The goal of the present work is to provide a novel method to synthesize amorphous Ni–B catalyst with superior catalytic activity. Generally, electroless nickel films should have a uniform, compact appearance without visible defects such as pores, pits and cracks.[22] However, such an appearance is not suitable for the active component of a catalyst which has good dispersion and abundant defects. In 1980s, the metal-supported amorphous Ni–P catalyst had been prepared by EN plating,[23] which was improved and then employed to the hydrogenation of benzaldehyde.[24,25] Recently, the preparation of metal-coated nanopartices has been reported using this technology owing to its particular advantage in directing the deposition of metal.[26] Here, we report a method to prepare a porous and well-dispersed amorphous Ni–B catalyst on titania powder by silver-catalyzed EN plating technology, as metal silver is a suitable catalyst for electroless Ni–B deposition and more economical than conventional metal palladium.[27–30] Without the presence of stabilizer in the EN plating solution, certain titania supported with a little amount of silver was transferred into the plating solution and catalyzed the plating solution. In the initial stage of EN plating, ever increasing nickel nuclei on the surface formed by the catalysis of silver. Then these nickel nuclei accelerated the rapid deposition of amorphous Ni–B clusters over them to compose porous Ni–B

Institute of New Catalytic Materials Science, College of Chemistry, Nankai University, Tianjin, 300071, P.R. China.
E-mail: zhangmh@nankai.edu.cn; Fax: +86 22 2350 7730;
Tel: +86 22 2350 7730

† Electronic supplementary information (ESI) available: Hydrogenation schemes and TEM micrographs and EDX spectrum of Ni–B/TiO_2 compounds. See DOI: 10.1039/b510975b

nanoparticles, due to the autocatalysis of nickel nuclei themselves. The resulting Ni–B/TiO_2 catalyst exhibited superior catalytic activity to that of conventional Ni–B/TiO_2 catalyst prepared by impregnation–reduction method.

Experimental

Preparation of Ni–B and Ni–B/TiO_2 catalysts

Commercially available solvents and reagents were used without further purification. Details of representative reactions are as following. Silver nitrate (0.02 g), ammonium hydroxide (0.15 g), sodium hydroxide (0.005 g) and formaldehyde (0.002 g) were dissolved in distilled water (425 ml).[31] Titania (6.39 g) was then transferred into the solution. After stirring at 313 K for 4.0 h, the resulting Ag/TiO_2 was washed with distilled water and dried at 363 K for 4.0 h. The EN plating solution consisted of nickelous sulfate (7.1 g L^{-1}), ethylenediamine (16.6 g L^{-1}), potassium borohydride (5.5 g L^{-1}), sodium hydroxide (40.0 g L^{-1}), and it was stable below 333 K. To prepare the supported Ni-B/TiO_2 catalyst, the Ag/TiO_2 precursor (3.0 g) was added into 150 mL as-prepared plating solution with stirring at 318 K. The reaction lasted about 35 min until no significant bubbles were observed. The resulting Ni–B(EN)/TiO_2 was washed thoroughly with distilled water until pH = 7, then washed with absolute alcohol to remove water and kept in absolute alcohol. In order to investigate the formation process of Ni–B(EN)/TiO_2 during plating, some intermediate samples were collected at the different plating time. The samples were washed and kept as above.

Bulk amorphous Ni–B alloy was synthesized by adding 5.0 mL 0.2 M silver nitrate aqueous solution into 150 mL as-prepared plating solution. For comparison, a conventional Ni–B(IR)/TiO_2 catalyst (20 wt%, theoretical Ni loading) was prepared by impregnation–reduction method.[32]

Characterization of catalysts

X-Ray diffraction patterns were collected on the Rigaku D/max-2500 diffractometer by using Ni-filtered Cu Kα radiation (λ = 1.5418 Å) at a scan rate of 2° min^{-1}. The transmission electron micrographs were carried out on the Philips EM400ST. The high-resolution transmission electron micrographs were imaged on a JEOL JEM 2010FEF device equipped with an EDX system. Samples for TEM were prepared by placing a drop of the sample suspension on a copper grid coated with carbon film. The chemical composition of the sample was determined by inductively coupled plasma (ICP) analysis using an IRIS Advantage spectrometer. SEM images were obtained on a LEO 1530VP field emission instrument. The surface area was measured using the BET method by N_2 physisorption at 373 K on the automatic surface area and pore size analyzer (Autosorb-1-MP 1530VP). The nickel surface area was determined from hydrodesulfurization of 3-methylthiophene in the liquid phase.[33–35]

Hydrogenation of sulfolene and 1,3-dimethyl-5-nitroso-6-aminouracil (DMNAU)

Hydrogenation of sulfolene (Scheme S1 in the electronic supplementary information (ESI)†). The hydrogenation of sulfolene was carried out in a high-pressure stainless steel autoclave. In a typical experiment, 0.7 g catalyst was dispersed in 30 ml distilled water, 30 g sulfolene was transferred to the solution. After replacing the air with H_2 in the reactor, the reaction was performed at 328 K and 3.0 MPa of hydrogen pressure with stirring at 500 rpm for 2 h. The hydrogenation product was filtered to remove the solid catalyst and analyzed by a gas chromatograph equipped with a flame ionization detector (FID).

Hydrogenation of 1,3-dimethyl-5-nitroso-6-aminouracil (DMNAU) (Scheme S2 in the ESI†). The reaction was carried out in a high-pressure stainless steel autoclave. A 0.9 g amount of catalyst was mixed with 10.5 g DMNAU and 69 ml distilled water. After replacing the air with H_2 in the reactor, the reaction was performed at 333 K and 0.4 MPa of hydrogen pressure with stirring at 800 rpm for 4.0 h. The hydrogenation product was analyzed by chemical titration.

Results and discussion

For comparison, the supported catalysts were prepared with a similar load of active metal, nickel (Table 1). We have noticed that there is a little difference of atomic ratio in both Ni–B/TiO_2 catalysts, which can be ascribed to the different preparation method. [13,19] XRD patterns of Ni–B alloy were recorded in 2θ from 30 to 80°. The broad and featureless peak (around 2θ = 45° in Fig. 1b) is caused by the amorphous structure of Ni–B particles[12,32] and diffraction peak (2θ = 38.2° in Fig. 1b) is due to the presence of silver. However, both Ni–B/TiO_2 samples (Fig. 1a), are completely the same and the only diffraction lines are due to the presence of anatase TiO_2. It is the result of good dispersion of Ni–B particles on the support and the weak diffraction signal of amorphous Ni–B alloy.[36]

The nature of the alloy particles was confirmed by various techniques other than XRD, including SEM, TEM, SAED and BET. A scanning electron micrograph of catalyst showed homogeneous dispersed, spherical Ni–B nanoparticles anchored on support (Fig. 2a). However, web-like aggregates (rectangles in Fig. 2b) coated on the TiO_2 support were presented in Ni–B(IR)/TiO_2, which should be due to ultrafine

Table 1 Chemical composition and catalytic activity of Ag/TiO_2 and Ni–B/TiO_2 catalysts

Sample	Metal loading (wt%)	S_{BET}/m^2 g^{-1}	S_{Ni}/m^2 g^{-1}	Composition of Ni–B (atomic ratio)	Conversion of sulfolene (%)	Conversion of DMNAU (%)
Ag/TiO_2	0.15 (Ag)	18.3	0	—	0.1	0
Ni–B(EN)/TiO_2	9.81 (Ni)	22.5	5.4	$Ni_{66.5}B_{33.5}$	79.5	94.8
Ni–B(IR)/TiO_2	9.94 (Ni)	23.2	2	$Ni_{62.3}B_{37.7}$	37.2	61.5

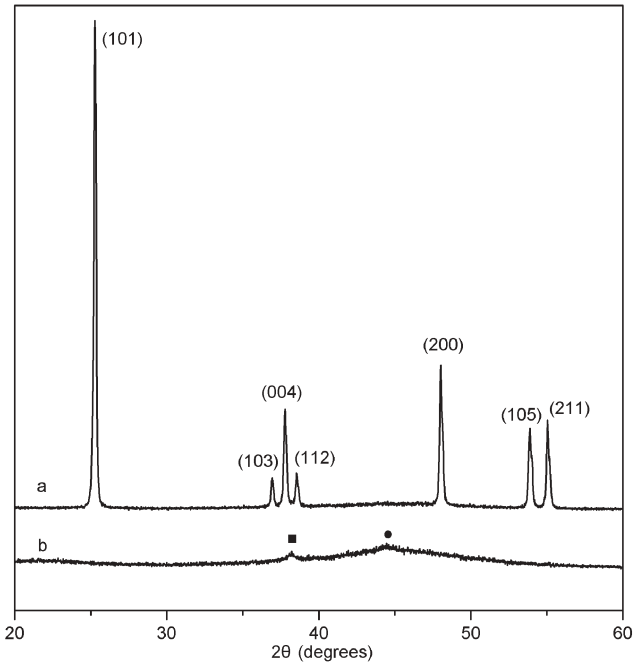

Fig. 1 XRD patterns of (a) Ni–B/TiO_2 and (b) bulk Ni–B.

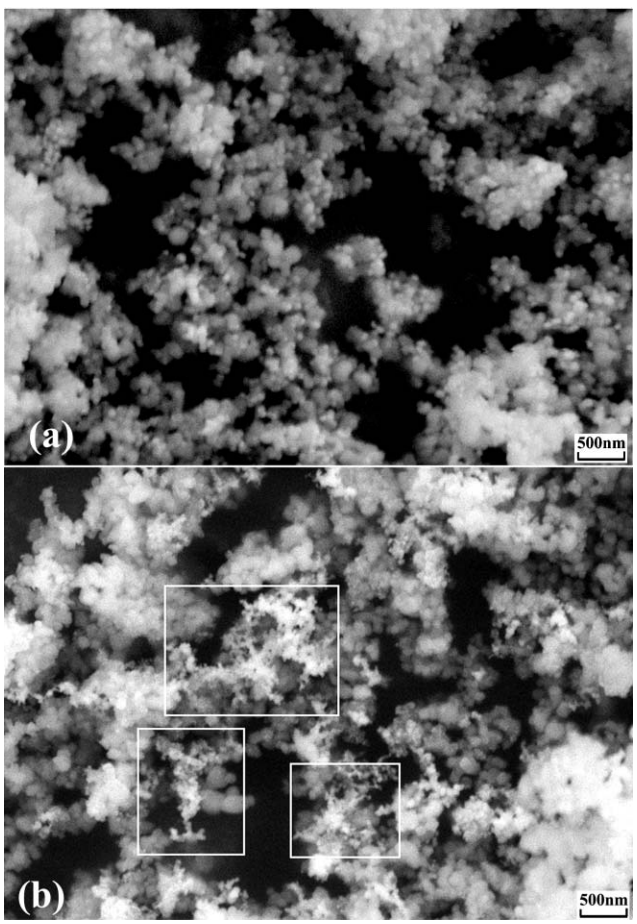

Fig. 2 SEM micrographs of (a) Ni–B(EN)/TiO_2 and (b) Ni–B(IR)/TiO_2.

Ni–B particles.[38] During the preparation of supported Ni–B(IR)/TiO_2 by impregnation–reduction method,[37] we have observed the homogeneous distribution of Ni–B particles at the lower Ni loading. With the increasing of the content of nickelous ions absorbed by the support, parts of nickelous ions will be inevitably diffused into the solution during the reduction. Finally, the dissociative Ni–B particles formed in the solution and then agglomerated and deposited on the support (Fig. S1 in the ESI†). The SEM studies confirm that amorphous Ni–B particles prepared by silver-catalyzed EN plating method are distributed homogeneously over the surface of TiO_2, without Ni–B nanoparticles agglomerating on the support. Further more, although the particle size of Ni–B particles in Ni–B(EN)/TiO_2 is much larger than that of Ni–B(IR)/TiO_2 (Fig. S1 in the ESI†), the S_{Ni} is still much higher, which suggests that the exposure of active nickel on the surface can be improved by silver-catalyzed EN plating (Table 1). The results agreed with the surface of Ni–B particles being mostly covered by boron in the amorphous Ni–B alloy prepared from chemical reduction.[33]

A transmission electron micrograph of Ni–B(EN)/TiO_2 sample is shown in Fig. 3. Spherical Ni–B particles with a size in the range of 30–50 nm are homogenously dispersed on TiO_2 particles. Unlike the solid sphere of conventional Ni–B particles (Fig. S1 in the ESI†),[14,37] Ni–B nanoparticles prepared by silver-catalyzed EN plating formed flower-like features with radiused capillary pores. To investigate the morphology of Ni–B(EN)/TiO_2 sample, one of Ni–B nanoparticles was characterized by HRTEM and SAED. Fig. 4a shows that the Ni–B particle contains many pores from inner nuclear to exterior surface. In the magnified Fig. 4b, it is clear that the Ni–B particle contains a 5 nm nuclear and 1–1.5 nm porous. Even though Ag metal is present, no spots or even diffraction rings exist due to Ag were found in the selected electron diffraction (SAED) pattern of Ni–B particles (inset of Fig. 4b), which confirms that the as-prepared Ni–B/TiO_2 catalyst by silver-catalyzed EN plating exhibits the amorphous structure. The inset of the HRTEM image of Ni–B in Fig. 4b shows that no lattice fringes can be found, in agreement with the lack of long-range ordering nature in amorphous materials. Short-range ordering structures possibly exist and

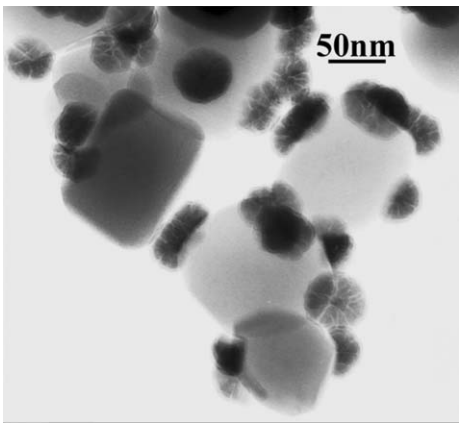

Fig. 3 TEM micrograph of Ni–B(EN)/TiO_2 catalyst.

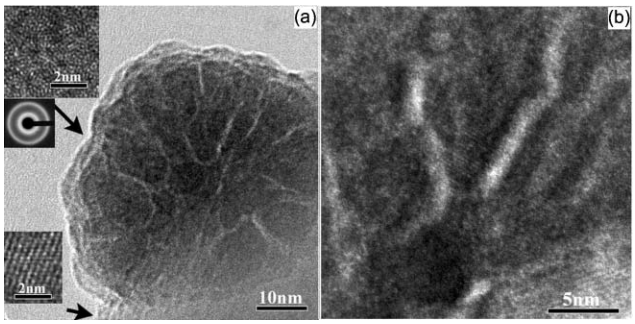

Fig. 4 HRTEM micrographs of (a) Ni–B(EN)/TiO_2 catalyst and (b) the center of Ni–B particle. Insets: the corresponding SAED pattern of Ni–B and HRTEM images of Ni–B particle and TiO_2.

are demonstrated by the other literature.[39] For the HRTEM image of crystallized TiO_2 support, the visible lattice spacing with 3.52 Å is in good agreement with the *d*-spacing values for {101} crystallographic planes of anatase measured by X-ray diffraction.

Process of silver-catalyzed EN plating

For the rest of the paper we concentrate on the process of silver-catalyzed EN plating. Two stages, the nucleation stage (ignition phase) and growth stage (agitation phase), are investigated. The nucleation stage lasts about 12 min accompanied with the release of little hydrogen and the gradually-changing gray color of the solid; while during the growth stage, mass bubbles emerge sharply with sequential deposition of black Ni–B particles on titania until the reaction was finished after 35 min. From literature data, it appears that the whole electroless deposition shows two different behaviours before growth stage. During the nucleation stage, when the first nickel nuclei takes place on the surface, the agitation has a great influence on reaction rates throughout the mass transfer enhancement and the cleaning effects of the catalysts (Pd or Ag). After the deposition of adequate nuclei on the surface, the reaction is controlled by the autocatalytic properties of the nickel.[19] The investigation of formation process of porous Ni–B particles, as measured by electron microprobe, were performed by analysis of some intermediate samples at the different plating time.

The TEM image of as-synthesized Ag/TiO_2 with 0.15 wt% loading is shown in Fig. 5a. Tiny silver clusters (black spots) are distributed randomly over titania, ranging from 8 to 10 nm in diameter. Alternatively, most surfaces of titania remain free of silver deposits. After plating for 8 min and 12 min (Fig. 5b and 5c), silver clusters were coated with deposited nickel clusters and grew to 15–20 nm. Simultaneously, some new nickel clusters (confirmed by EDX (Fig. S2 in the ESI†)) over titania are present near silver clusters. The results showed clearly that silver plays a major role during the nucleation step. Hydrogen is adsorbed onto silver to decrease the presence of hydrogen in solution, and therefore decreases the competition between the reduction of nickelous ions and the reduction of hydrogen.[40] This would lead to an increase in plating rate at the beginning of the deposit. At the same time, more nickel nuclei would be formed on the surface and mechanical anchoring of the nickel in the fine pits on the resin surface would be favoured. Flis and Duquette[20] and Hong *et al.*[41] also indicated that the initial deposition of nickel is not only confined to the active metals, but also a part of nickel clusters will be diffused into the solution and be adsorbed by the passivation surface of substrate. Therefore, the reduced nickel atoms in the nucleation stage mainly turn into detached nickel clusters and are absorbed by titania to form new catalytic nuclei when the stabilizer does not exist,[41] for which the nickel nuclei distributed homogeneously over TiO_2. With the increasing plating time in the nucleation stage, more and larger nickel nuclei appear with the size of 5–10 nm (Fig. 5c). As the EN plating is an autocatalytic reaction, abundant nickel nuclei

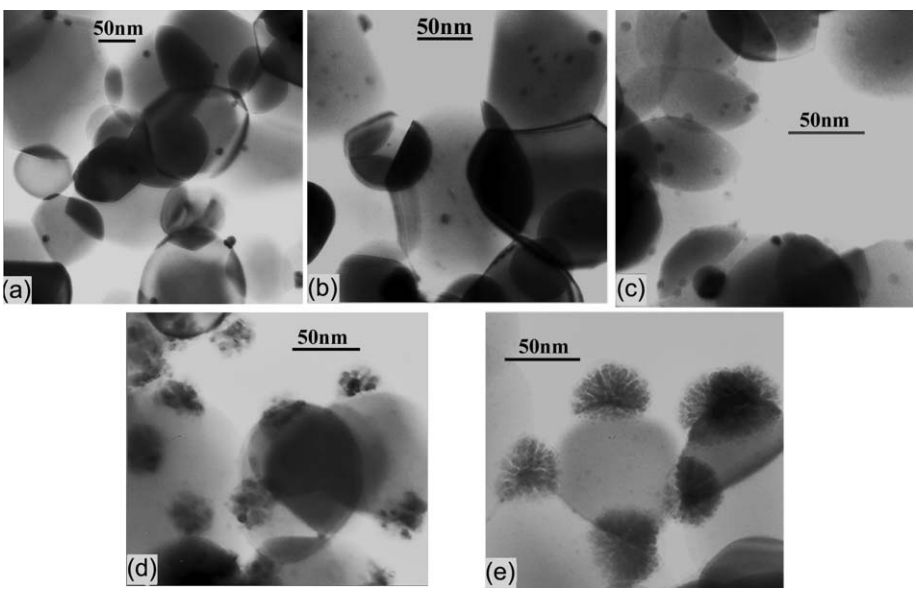

Fig. 5 TEM micrographs of the intermediate Ni–B(EN)/TiO_2 samples at the different plating time (a) Ag/TiO_2, (b) 8 min, (c) 12 min, (d) 18 min and (e) 28 min.

accelerate the deposition of nickel from the plating solution with lots of bubbles released. Then, the plating turns to the growth stage, mass nickel atoms carrying partial boron atoms mainly packed over nickel seeds (Fig. 5d). By the way, the packing process of nickel is accompanied by the generation of a large amount of hydrogen at the interface of nickel clusters and plating solution, in which the passages formed by the releasing of hydrogen and finally shaped the porous features of 30–40 nm Ni–B particles (Fig. 5d and 5e). The early studies on the electroless Ni–P deposition have suggested that preliminary deposition of small amounts of nickel results in a discontinuous and porous layer.[20] In our present experiment, we found it is feasible to design porous supported amorphous Ni–B/TiO_2 catalyst. The results indicate that the size of Ni–B particles can be easily controlled through changing the Ni loading rates according to silver-catalyzed plating method.

Hydrogenation activity

Hydrogenation of sulfolene to sulfolane and hydrogenation of 1,3-dimethyl-5-nitroso-6-aminouracil (DMNAU) to 1,3-dimethyl-5,6-diaminouracil (DMDAU) (Schemes S1 and S2 in the ESI†) are carried out without the diffusion effects. Both reactions are used to measure the initial catalytic activities of supported Ni–B/TiO_2 catalysts. The conversions of sulfolene and DMNAU over Ni–B(EN)/TiO_2 and Ni–B(IR)/TiO_2 catalysts are respectively listed in Table 1. Blank experiment indicates that Ag/TiO_2 precursor has a negligible effect on the reactions, but catalytic activities of Ni–B(EN)/TiO_2 catalyst for both reactions are much higher than those of Ni–B(IR)/TiO_2 catalyst at the same reaction conditions. Although the load of nickel is identical between Ni–B(EN)/TiO_2 and Ni–B(IR)/TiO_2, the S_{Ni} of Ni–B(EN)/TiO_2 are higher than that in Ni–B(IR)/TiO_2, which is certainly due to the unique porous structure and homogeneous dispersion of Ni–B nanoparticles on TiO_2 support. The supported amorphous Ni–B(EN)/TiO_2 catalyst exhibits superior catalytic activity, because of the more catalytic active sites on the surface than conventional Ni–B(IR)/TiO_2 catalyst,.

Conclusions

In the present work, silver-catalyzed EN plating yields amorphous, porous and flower-like Ni–B alloy particles. The investigation of the process of plating is illustrated by TEM in detail. The result suggests the growth and distribution of Ni–B particles can be controlled by the catalysis of silver. Hydrogenation data indicate the superior catalytic nature of the as-prepared amorphous Ni–B(EN)/TiO_2 catalyst. This result shows that it is a novel method to prepared porous supported amorphous Ni–B alloy catalyst, which can expose more homogeneous active sites on the surface of catalyst. It is predicted that other supported amorphous alloy catalysts, such as Co–B, Fe–B, Ni–Co–B, *etc*, can be realized by corresponding electroless plating method.

Acknowledgements

The present work was partly supported by NSF of China (20403009 and 20233030), Key Project of Chinese Ministry of Education. (105045), and Open Foundation of State Key Laboratory of Heavy Oil Processing.

References

1 *Metallic Glasses: Production, Properties and Applications*, ed. T. R. Anantharaman, Trans Tech Publications, Aedermannsdorf, Switzerland, 1984.
2 P. Haasen and R. I. Jaffe, *Amorphous Metals and Semiconductors*, Pergamon, London, 1986.
3 N. F. Motte and E. A. Davis, *Electronic Processes in Non-Crystalline Materials*, Clarendon Press, Oxford, 1979.
4 H. Steeb and H. Warlimont, *Rapidly Quenched Metals*, Elsevier, Amsterdam, 1985.
5 J. Van Wonterghem, S. Morup, C. J. W. Koch, S. W. Charles and S. Wells, *Nature*, 1986, **322**, 622.
6 A. Molnar, G. V. Smith and M. Bartok, *Adv. Catal.*, 1989, **36**, 329.
7 R. P. Messmer, *Phys. Rev. B: Condens. Matter*, 1981, **23**, 1616.
8 J. A. Schwarz, C. Contescu and A. Contescu, *Chem. Rev.*, 1995, **95**, 477.
9 Y. D. Wang, X. P. Ai and H. X. Yang, *Chem. Mater.*, 2004, **16**, 5194.
10 W. L. Dai, H. X. Li, Y. Cao, M. H. Qiao, K. N. Fan and J. F. Deng, *Langmuir*, 2002, **18**, 9605.
11 J. F. Deng, H. X. Li and W. J. Wang, *Catal. Today*, 1999, **51**, 113.
12 H. X. Li, H. Li, W. L. Dai and M. H. Qiao, *Appl. Catal., A*, 2003, **238**, 119.
13 E. Z. Min and Ch. Y. Li, *Base of Science and Engineering of Green Petrochemical Technology*; Chinese Petrochem Press, Beijing, 2002.
14 X. Y. Chen, S. Wang, J. H. Zhuang, M. H. Qiao, K. N. Fan and H. Y. He, *J. Catal.*, 2004, **227**, 419.
15 J. Li, M. H. Qiao and J. F. Deng, *J. Mol. Catal. A: Chem.*, 2001, **169**, 295.
16 J. Y. Shen, Zh. Y. Li, Q. J. Yan and Y. Chen, *J. Phys. Chem.*, 1993, **97**, 8504.
17 A. Brenner and G. Riddell, *J. Res. Natl. Bur. Stand. (U.S.)*, 1946, **37**, 31.
18 H. G. Schenzel and H. Kreye, *Plat. Surf. Finish.*, 1990, **77**, 54.
19 G. O. Mallory and J. B. Hajdu, *Electroless Plating: Fundamentals and Applications*, American Electroplaters and Surface Finishers Society, Orlando, FL, 1990.
20 J. Flis and D. J. Duquette, *J. Electrochem. Soc.*, 1984, **131**, 51.
21 T. Homma, T. Yamazaki and T. Osaka, *J. Electrochem. Soc.*, 1992, **139**, 732.
22 T. S. N. Sankara Narayanan and S. K. Seshadri, *J. Alloys Compd.*, 2004, **365**, 197.
23 A. Yokoyama, H. Komiyama, H. Inoue, T. Masumoto and H. M. Kimura, *J. Catal.*, 1981, **68**, 355.
24 J. F. Deng, X. P. Zhang and E. Z. Min, *Appl. Catal., A*, 1988, **37**, 339.
25 H. X. Li, H. Li, W. J. Wang and J. F. Deng, *J. Catal.*, 2000, **194**, 211.
26 I. Lee, P. T. Hammond and M. F. Rubner, *Chem. Mater.*, 2003, **15**, 4583.
27 N. R. Jana, T. K. Sau and T. Pal, *J. Phys. Chem. B*, 1999, **103**, 115.
28 T. Ung, L. M. Liz-Marzán and P. Mulvaney, *J. Phys. Chem. B*, 1999, **103**, 6770.
29 W. Gang, Z. Hualan, L. Zhiguo, S. Yonghai, W. Li, S. Lanlan and L. Zhuang, *J. Phys. Chem. B*, 2005, **109**, 8739.
30 D. L. Van Hyning and C. F. Zukoski, *Langmuir*, 1998, **14**, 7034.
31 Y. D. Yin, Z. Y. Li, Z. Y. Zhong, B. Gates, Y. N. Xia and S. J. Venkateswaran, *J. Mater. Chem.*, 2002, **12**, 522.
32 L. J. Wang, W. Li, M. H. Zhang and K. Y. Tao, *Appl. Catal., A*, 2004, **259**, 185.
33 K. Molvinger, M. Lopez and J. Court, *J. Mol. Catal. A: Chem.*, 1999, **150**, 267.
34 S. Sanè, J. M. Bonaier, J. P. Damon and J. Masson, *Appl. Catal.*, 1984, **9**, 69.
35 K. Molvinger, M. Lopez, J. Court and P. Y. Chavant, *Appl. Catal., A*, 2002, **231**, 91.

36 Y. C. Xie and Y. Q. Tang, *Adv. Catal.*, 1990, **37**, 1.
37 H. Yamashita, M. Yoshikawa, T. Funabiki and S. Yoshida, *J. Chem. Soc., Faraday Trans. 1*, 1985, **81**, 2485.
38 Y. G. He, M. H. Qiao, H. R. Hu, Y. Pei, H. X. Li, J. F. Deng and K. N. Fan, *Mater. Lett.*, 2002, **56**, 952.
39 A. M. Bratkovsky and A. V. Smirnov, *Phys. Lett. A*, 1990, **146**, 522.
40 F. Touyeras, J. Y. Hihn, S. Delalande, R. Viennet and M. L. Doche, *Ultrason. Sonochem.*, 2003, **10**, 363.
41 X. Yin, L. Hong, B. H. Chen and T. M. Ko, *J. Colloid Interface Sci.*, 2003, **262**, 89.